



Anthracene derived dinuclear gold(I) diacetylides complexes: Synthesis, photophysical properties and supramolecular interactions

Veenu Mishra ^a, Abhinav Raghuvanshi ^b, Anoop Kumar Saini ^a, Shaikh M. Mobin ^{a,*}

^a Discipline of Chemistry, Indian Institute of Technology Indore, Simrol, Indore 452020, India

^b Department of Chemistry, Indian Institute of Technology Bombay, Mumbai 400076, India



ARTICLE INFO

Article history:

Received 1 February 2016

Received in revised form

1 April 2016

Accepted 12 April 2016

Available online 14 April 2016

Keywords:

Anthracene

Gold(I) diacetylide

Fluorescence

Intermolecular Au···H–C interactions

ABSTRACT

New anthracene derived dinuclear Au(I)-diacetylides complex (**1**) has been synthesized in which two Au(I) units are attached at 9,10- positions of ethynyl anthracene moiety. **1** exhibits rare non-covalent intermolecular Au···H–C interactions, leading to the formation of a supramolecular 2D-network. Further, to understand the effect of C≡CAuPPh₃ units at different position, complexes (**2**) and (**3**) were synthesized, where C≡CAuPPh₃ units are attached to 2,6- and 1,8- positions of anthracene, respectively. The absorption and emission spectra of **1–3** have been studied and surprisingly **1** was found to be highly fluorescent with high quantum yield compared to **2** and **3**, this may be due to more perturbation of Au(I) on π system. Complexes **1–3** have been characterized by elemental analysis, NMR and Mass spectroscopy and authenticated by their single-crystal X-ray structures.

© 2016 Elsevier B.V. All rights reserved.

1. Introduction

Polyaromatic hydrocarbons (PAHs) with extended conjugation have gained much attention in past decades due to their strong visible π - π^* absorption, intense luminescence and high charge mobility in the solid state [1–3]. They have got applications in advanced materials for organic light-emitting diodes (OLEDs), field-effect transistors (FETs) and solar cells [4,5]. Connecting PAH to the metal center through the alkyne unit as a spacer introduces additional features to be used as molecular wires, nonlinear optical materials and molecular electronics [6–8]. It is well known that metallation of PAH ring system has significant effect on its photophysical properties and structural dimensionalities [9–14].

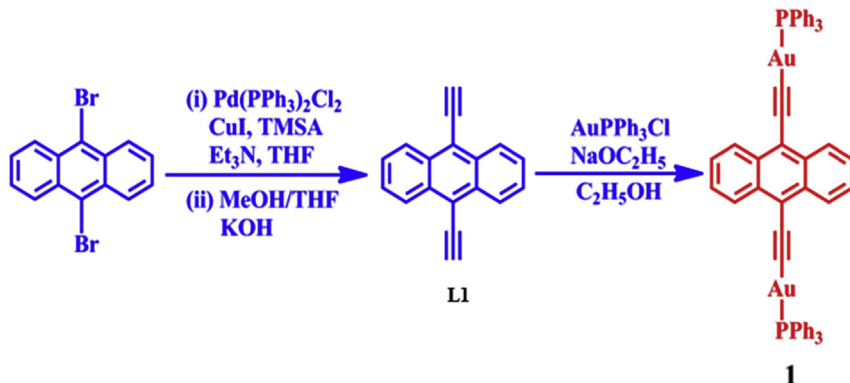
Alkynyl gold complexes have drawn considerable interest in recent years [15] because of their aurophilic properties, exciting photophysical properties and their ability to build supramolecular array [16,17]. Recent reports on PAH linked with platinum(II) and gold(I) via the alkynyl spacer show interesting structural property, photophysical properties and their structural reactivity [18–23]. The organo Au(I) system shows enhanced luminescent properties for alkynylAu(I) phosphines complexes compared to other gold complexes [24–33].

Non-covalent interactions are the primary driving force in constructing supramolecular architectures as well as in determining the constitution and conformation of molecules. Although, in gold chemistry extensive literature are available to understand the aurophilic interaction (Au···Au) [34], however, the non-covalent Au···H–C interactions are less explored [35–37]. The Au···H–C interactions are mainly observed in Au(I) phosphine and thione complexes where gold atoms are in almost linear geometry and leaving behind coordination site for gold hydrogen interactions. Usually, Au···H–C contacts in Au(I) complexes are intramolecular in nature and in case of intermolecular Au···H–C interactions they are restricted to supramolecular 1D-chain [38–48].

Herein we report the synthesis, characterization and photophysical properties of a series of three new anthrylAu(I) diacetylides, **1–3** complexes in which the Au(I) acetylides units are attached at 9,10-, 2,6- and 1,8-positions of anthracene. **1** display more red shift and stronger fluorescence with high quantum yield probably due to more perturbation of Au(I) on π system in **1** compared to **2** and **3**. Additionally, the single crystal studies of **1–3** reveal that **1** shows rare noncovalent intermolecular Au···H–C interactions that leads to the formation of a supramolecular 2D-network, whereas, in **3** intramolecular Au···H–C interactions have been observed.

* Corresponding author.

E-mail address: xray@iiti.ac.in (S.M. Mobin).

Scheme 1. Synthetic outline for **1**.

2. Results and discussion

1 was synthesized by reaction of 2 mol equivalent of PPh_3AuCl with ethynyl anthracene at 9,10-positions in presence of NaOEt in ethanol (Scheme 1). Compound **1** was characterized by various spectroscopic techniques. UV/Vis absorption and emission spectra of **1** reveals high fluorescence property with excellent quantum yield. Single crystal X-ray diffraction studies of **1**, indicate the existence of intermolecular $\text{Au}\cdots\text{H}-\text{C}$ interactions creating a supramolecular 2D-network.

1 was crystallized in $P2_1/n$ space group, with crystallographically imposed inversion center (Fig. 1 and Table S1). In **1**, the $\text{C}\equiv\text{CAuPPh}_3$ units are attached to the planar anthracene ring at the 9,10-positions. The $\text{Au}-\text{P}$ and $\text{Au}-\text{C}$ distances of $2.281(1)$ Å and $2.004(5)$ Å, respectively, are similar to that reported for aryl Au(I) phosphine complexes (Table S2) [49,50]. The slight deviation from linearity has been observed in $\text{P}-\text{Au}-\text{C}$ angle of $175.1(2)^\circ$ in **1**, consequently the $\text{C}\equiv\text{C}(\text{C}1-\text{C}2)$ bond lies 4° out of the anthracene plane.

It is interesting to note that the linear coordination geometry around Au(I) in **1** makes it susceptible for additional non-covalent interactions. The packing diagram of **1** reveals that the coordination environment of Au(I) is extended further by an intermolecular $\text{Au}\cdots\text{H}-\text{C}$ interaction between the metal ion and one of the aromatic hydrogens of PPh_3 of adjacent molecule $\text{Au}(1)\cdots\text{H}(11)-\text{C}(11)$ $2.87(1)$ Å with the $\text{Au}(1)\cdots\text{H}(11)-\text{C}(11)$ bond angle of $171.00(1)^\circ$. It has been observed that neighboring molecules link together through these interactions along the *b*-axis, yielding one-dimensional polymeric chain [51]. This 1D chain further extends via the same $\text{Au}\cdots\text{H}-\text{C}$ interactions along the *c*-axis, forming herringbone like 2D-network. Thus, both the gold atoms in **1** are involved in $\text{Au}\cdots\text{H}-\text{C}$ supramolecular interactions (Fig. 2, S1 and S2).

The considerably short $\text{Au}\cdots\text{H}-\text{C}$ bond distance and larger $\text{Au}\cdots\text{H}-\text{C}$ bond angle develop regular directionality, which suggest that these interactions are hydrogen bonding in nature [43–45]. To the best of our knowledge, **1** represents the first example of supramolecular 2D-network involving intermolecular $\text{Au}\cdots\text{H}-\text{C}$ non-covalent interactions.

The above interesting features show the influence (if any) of the binding of $\text{C}\equiv\text{CAuPPh}_3$ at the 9,10-positions of the anthracene moiety towards the formation of 2D-network via $\text{Au}\cdots\text{H}-\text{C}$ interactions. This prompted us to synthesized similar complexes by varying the position of alkynyl group attached to anthracene such as 2,6- and 1,8-positions. In this regard, we obtained compounds **2** and **3** with the linkage of $\text{C}\equiv\text{CAuPPh}_3$ at 2,6- and 1,8-positions (Scheme 2).

Complexes **2** and **3** were synthesized by following the same procedure as of **1** and along with usual spectroscopic techniques analysed by UV/Vis absorption/fluorescence spectra and were established to be fluorescent albeit less than **1**. Both compounds were further analysed by single crystal X-ray diffraction studies ensuing the presence of $\pi\cdots\pi$ and $\text{CH}\cdots\pi$ interactions in **2** while intramolecular $\text{Au}\cdots\text{H}-\text{C}$ interaction in **3**.

2 and **3** were crystallized in $P\bar{T}$ and $P2_12_12_1$ space group, respectively, (Figs. 3 and 4 and Table S1). **2** shows a planar

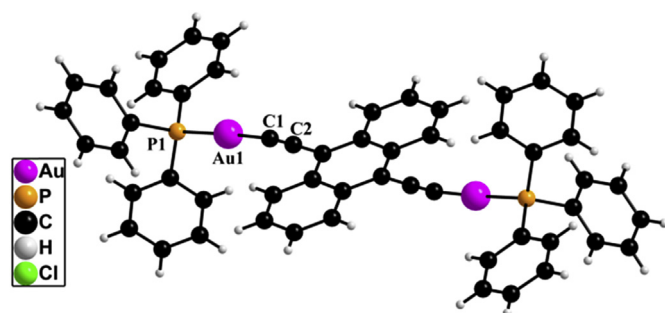


Fig. 1. Perspective view of **1**. (Solvent molecules are omitted for clarity). Selected bond distances (\AA) and bond angles (deg): $\text{Au}(1)-\text{P}(1)$ $2.281(3)$, $\text{Au}(1)-\text{C}(1)$ $2.004(5)$, $\text{P}(1)-\text{Au}(1)-\text{C}(1)$ $175.1(2)$, $\text{Au}(1)-\text{C}(1)-\text{C}(2)$ $173.7(4)$.

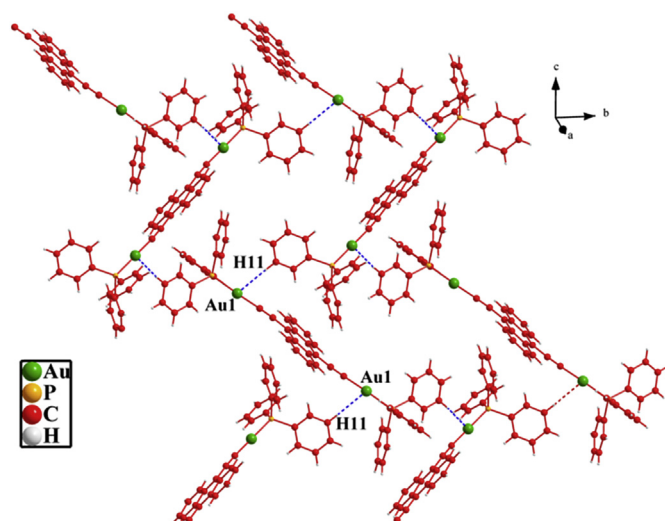
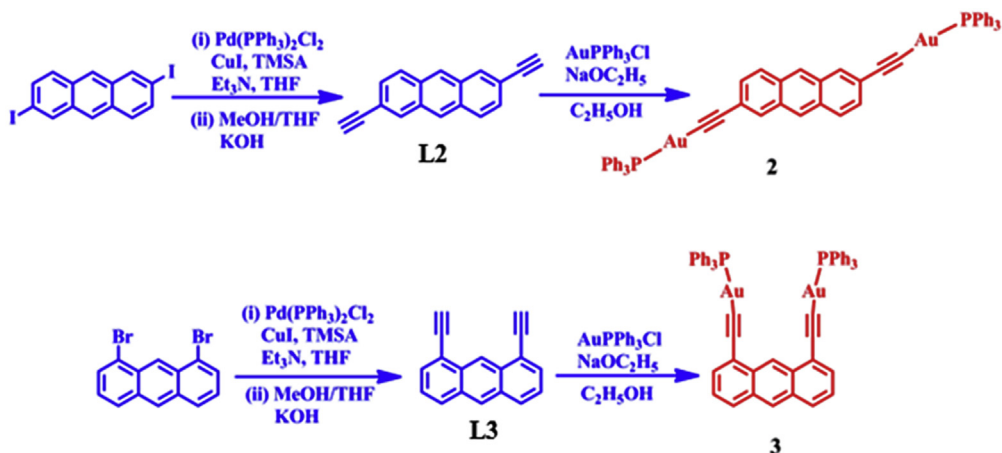
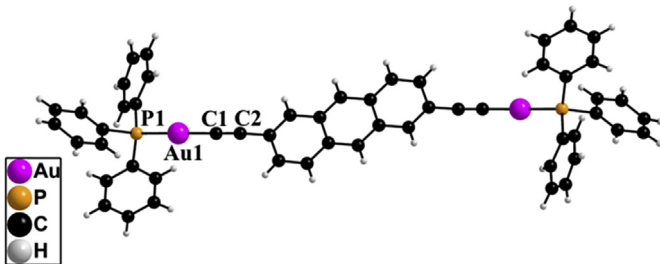
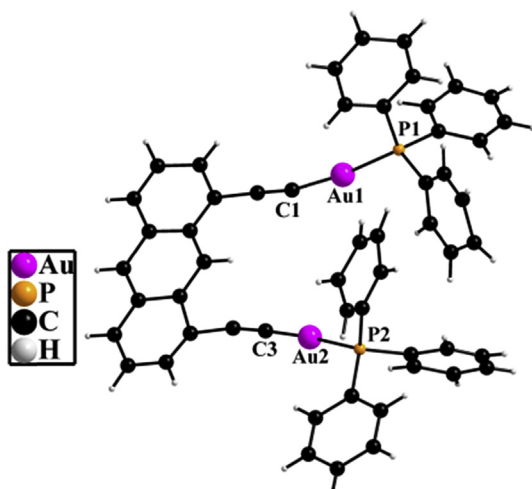


Fig. 2. $\text{Au}\cdots\text{H}-\text{C}$ bonded supramolecular 2D network of **1** through tilted *a* axis.

Scheme 2. Synthetic outlines for **2** and **3**.Fig. 3. Perspective view of **2**. Selected bond distances (\AA) and bond angles (deg): Au(1)–P(1) 2.277(5), Au(1)–C(1) 2.03(3), P(1)–Au(1)–C(1) 176.8(6), Au(1)–C(1)–C(2) 172.4(17).

anthracene ring on which $\text{C}\equiv\text{CAuPPh}_3$ units are attached to its 2,6-position. Unlike **2**, where substitutions were at *trans* positions, in **3**, the $\text{C}\equiv\text{CAuPPh}_3$ units are attached to its 1,8- position i.e. *cis*-position to the planar anthracene ring. The distance between Au–P and Au–C are 2.275(5) \AA , 2.00(2) \AA in **2**, and 2.271(7) \AA , 2.282(6) \AA , 1.94(3) \AA , in **3** respectively (Table S2). Which are similar to the reported arylAu(I) phosphine complexes. The P–Au–C and

Fig. 4. Perspective view of **3**, distances (\AA) and bond angles (deg): Au(1)–P(1) 2.271(7), Au(2)–P(2) 2.282(6), Au(1)–C(1) 1.94(3), Au(2)–C(3) 1.94(3), C(1)–C(2) 1.21(3), C(3)–C(4) 1.23(3); P(1)–Au(1)–C(1) 173.0(6), P(2)–Au(2)–C(3) 175.7(9), Au(1)–C(1)–C(2) 168.1(19), Au(2)–C(3)–C(4) 169(2).

Au–C–C angles in **2** were found to be 176.9(4) $^\circ$ and 172.4(17) $^\circ$ which suggest slightly distorted geometry around Au(I) from linearity. The $\text{C}\equiv\text{C}(\text{C}1–\text{C}2)$ bonds in **2** and **3** were also slightly deviated from the anthracene plane by 5 $^\circ$ and 2 $^\circ$, respectively. Compound **3** found to be highly strained due to the presence of bulky PPh₃ groups at *cis* position which results both the Au(I) centers to move slightly outward and tilted from the anthracene plane (Table S2).

The packing diagram of **2** reveals the existence of $\text{CH}\cdots\pi$ and $\pi\cdots\pi$ interactions. $\text{CH}\cdots\pi$ interactions involve H(13) of phenyl ring of PPh₃ unit and π electrons of acetylenic bond, forming a wave like 1D polymeric chain (Fig. 5 and S3). The packing features of **3** establishes intramolecular Au–H–C interactions involving hydrogens of PPh₃, where Au–H–C bond distances and bond angles are Au(2)–H(48) 3.01(1) \AA , Au(2)–H(54) 2.86(1) \AA , Au(1)–H(20) 3.00(1) \AA and Au(2)–H(54)–C(54) 123.00(1) $^\circ$, Au(2)–H(48)–C(48) 118.31(1) $^\circ$, Au(1)–H(20)–C(20) 111.66(1) $^\circ$ (Fig. 6).

Unlike **1** or **2**, the observed intramolecular Au–H–C interactions in **3**, originate due the *cis* orientation of $\text{C}\equiv\text{CAuPPh}_3$ moieties. The steric repulsion between the two PPh₃ groups in the *cis* orientation facilitates the C–H of the phenyl ring to move closer to the gold. The packing of **3** is further extended by C–H– π , interactions C(4)–H(34)– π 3.359 \AA , resulting in 1D polymeric chain (Fig. 7, and S4). The synthesis of **3** found to be unique, as to the best of our knowledge there are no reports of 1,8-anthracyl complexes with bulky PPh₃ group substitution at Au(I) center. So far only few reports of 1,8-anthracyl substituted Pd(II)/Pt(II) complexes with less bulkier triethyl phosphine group at Pd(II) center have been reported [52–55].

The absorption and emission spectroscopic studies of complexes **1–3** and their respective ligands were recorded in CH_2Cl_2 (1.0×10^{-5} M) at room temperature (Figs. 8 and 9, S5–S6 and Table 1, S3). **1–3** complexes display two absorption bands (i) with a broad intense vibronic band between 320 and 470 nm (A), and (ii) very intense, band between 265 and 310 nm (B). Since the spectra of anthracene and diethynyl anthracene display similar absorption patterns, the absorption bands are assigned to $\pi\rightarrow\pi^*$ transitions primarily localized in the anthracene. The absorption bands of anthracene are due to the $\text{LUMO}\leftarrow\text{HOMO}\left({}^1\text{B}_{1u}\leftarrow{}^1\text{Ag}\right)$, $\text{LUMO}\leftarrow\text{HOMO}-1\left({}^1\text{B}_{2u}\leftarrow{}^1\text{Ag}\right)$, $\text{LUMO}+1\leftarrow\text{HOMO}\left({}^1\text{B}_{2u}\leftarrow{}^1\text{Ag}\right)$, The second and third transitions lead to the two degenerate ${}^1\text{B}_{2u}$ excited states, which undergo strong configuration interaction to give the high-energy “plus” state ${}^1\text{B}_{2u}^+$ and the low-energy “minus” state ${}^1\text{B}_{2u}^-$. The very intense band at around 250 nm corresponds to the $({}^1\text{B}_{1u}\leftarrow{}^1\text{Ag})$ transition. Whereas the transition $({}^1\text{B}_{1u}\leftarrow{}^1\text{Ag})$ is slightly higher in energy than the

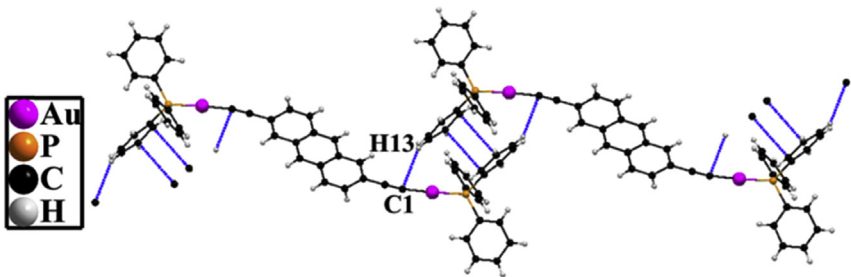


Fig. 5. Wave like 1D polymeric chain of **2** showing CH- π and π - π interactions.

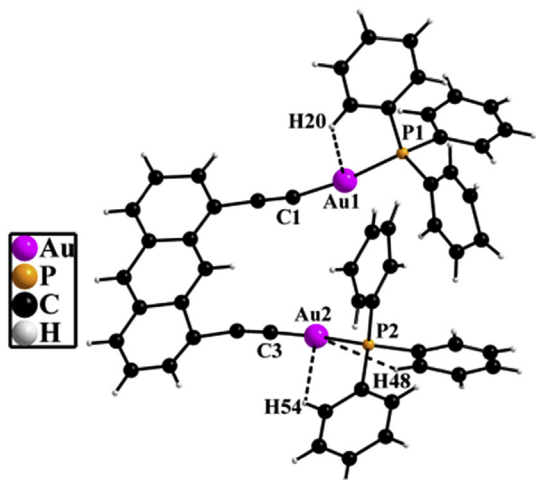


Fig. 6. Intramolecular Au···HC interactions in **3**.

(${}^1\text{B}_{1\text{u}} \leftarrow {}^1\text{Ag}$) transition (${}^1\text{B}_{1\text{u}}$ is lower than ${}^1\text{B}_{2\text{u}}$ by $\sim 1500 \text{ cm}^{-1}$) is forbidden ($\epsilon \approx 10 \text{ M}^{-1} \text{ cm}^{-1}$) and hidden under the latter [10, 56].

Though the symmetries of the Au(I) complexes and anthracene are quite different, still there exist a similarity between absorption bands displayed by the complexes and the electronic transitions of anthracene. Band A in the spectra of the complexes corresponds to the LUMO \leftarrow HOMO (${}^1\text{B}_{1\text{u}} \leftarrow {}^1\text{Ag}$) transition, which is also known as an S0 \rightarrow S1 transition. The intense band B correspond to the transition to the “plus” state ${}^1\text{B}_{2\text{u}}^{\pm}$ (${}^1\text{B}_{2\text{u}}^{\pm} \leftarrow {}^1\text{Ag}$).

The transition is significantly intensified in the spectra of the complexes, indicating that the electronic structure of the anthracenyl ring is significantly perturbed by the Au(I) ions and the ethynyl groups [10, 57]. Further, absorption bands of complexes **1**, **2** and **3** are found to be red shifted compared to respective ligands.

Absorption maxima of **1** shows red shifts of $\sim 50 \text{ nm}$ compare to **2** and **3**, which indicates that substituents have more perturbation on the anthracenyl rings when they are at 9,10 position. In case of **2** and **3** the bands are observed almost in the same range. In addition to this, complexes display intense absorption in near-UV region. **2** shows a intense absorption band at 310 nm whereas in **1** and **3** show around 274 and 267 nm, similar to that of previously reported complexes [12].

Complexes **1**–**3** were found to be emissive in solution as their respective ligands. On excitation of complexes **1**, **2** and **3** at 434 nm, 389 nm and 398 nm, respectively, they display similar emission pattern to their corresponding ligands (Fig. 9 and S6. Table S3). The fluorescence of the complexes **1** and **3** were found to be red shifted from their respective ligands around 15–20 nm while marginal blue shift (5 nm) is observed in complex **2**. Emission spectra of **1** shows very strong fluorescence with quantum yield of 0.89 compared to **2** and **3** (quantum yield = 0.02 for **2** and 0.04 for **3**). **1** shows high fluorescence probably due to the substitution at 9,10 position which is in contrast with **2** and **3** [58, 59]. Complex **1** also shows emissive nature in solid-state (Fig. S7).

To get an insight into the nature of electronic transitions, density-functional theory (DFT) and time dependent density-functional theory (TDDFT) calculations were performed with the Gaussian09 program package [60]. All the calculations were performed at B3LYP [61, 62] level of theory using the Stuttgart/Dresden effective core potential (SDD) basis set [63] for the gold atoms and 6-31G** basis set [64] for remaining atoms. Geometries were optimized without imposed symmetry or other restraints. On the basis of the ground state optimized geometries, TD-DFT calculations were performed in presence of dichloromethane using the conductive polarizable continuum model (CPCM) [65, 66].

In all three cases, the calculated bond distances for the optimized structures are in good agreement to those obtained in their crystal structures (Figs. S8–S10). For all three complexes, the highest-occupied molecular orbitals (HOMOs) are π -type MOs

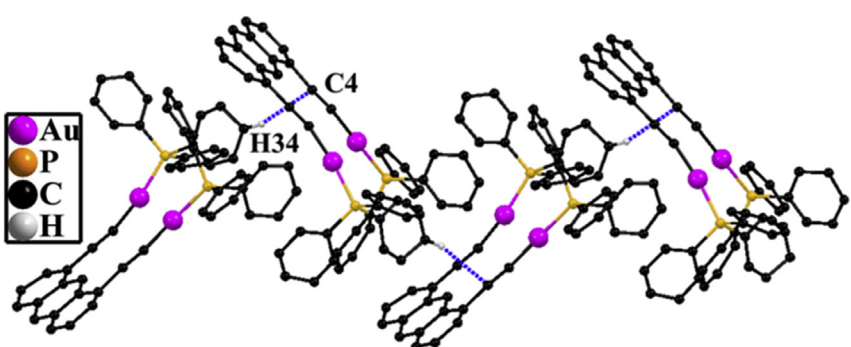


Fig. 7. 1D chain of **3** showing CH- π interactions.

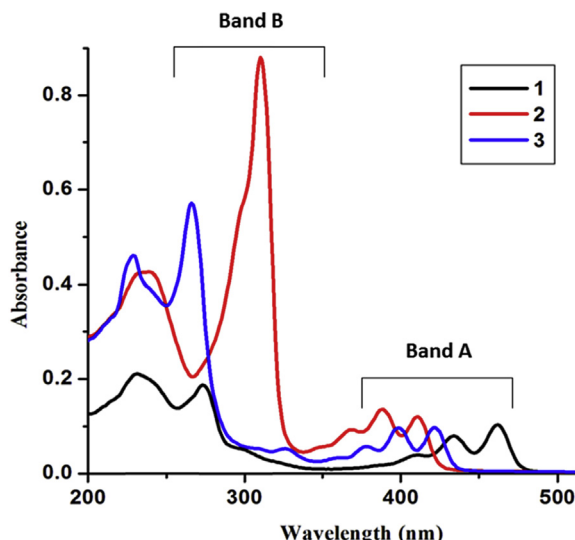


Fig. 8. Electronic absorption spectra of complexes (**1–3**) in CH_2Cl_2 .

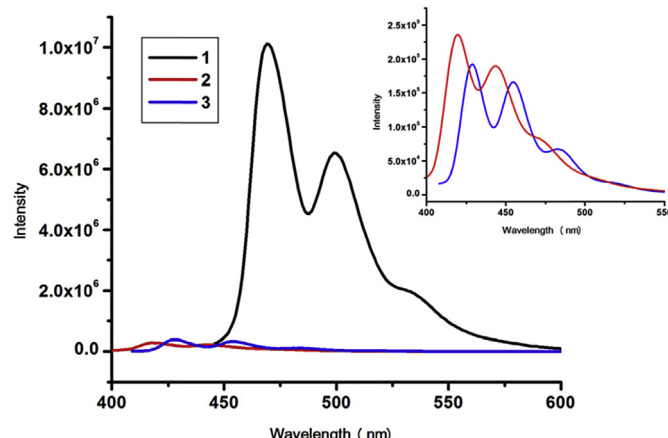


Fig. 9. Emission spectra of complexes (**1–3**) in CH_2Cl_2 . Inset shows the expanded emission spectra of **2** and **3**.

while the lowest-occupied molecular orbitals (LUMOs) are π^* -type, delocalized on the anthracene unit. The TD-DFT predicted spectra are in good agreement with the experimental data and clearly suggest that the band observed in the visible range is dominated by HOMO to LUMO excitation (Fig. S11). Further, in comparison to 2,6- and 1,8- derivative, there is red-shift in case of 9,10- anthracene derivative, which is supported by calculations as the calculated HOMO-LUMO gaps are 0.102 eV, 0.117 eV and 0.115 eV for **1**, **2** and **3** respectively (Fig. 10 and S11). Since perturbation on anthracene lower the symmetry of the π -system which leads to a bathochromic shift in HOMO to LUMO transition, the results suggest that substituents have more perturbation on the anthracenyl rings when they are at 9,10 position.

3. Conclusion

In summary, complex **1** with $\text{C}\equiv\text{CAuPPh}_3$ moieties attached to the 9,10-positions of anthracene selectively yields the strong fluorescent, rare 2D-network feature *via* intermolecular $\text{Au}\cdots\text{H}\cdots\text{C}$ interactions. However, the analogous compounds **2** and **3** with $\text{C}\equiv\text{CAuPPh}_3$ moieties attached to the 2,6- and 1,8- positions of anthracene result in weakly fluorescent 1D-polymeric chain *via* $\text{C}\cdots\text{H}\cdots\pi$ and $\pi\cdots\pi$ interactions and intramolecular $\text{Au}\cdots\text{H}\cdots\text{C}$ interactions, respectively. The present work thus highlights the $\text{Au}\cdots\text{H}\cdots\text{C}$ interactions as well as the impact of linkage of Au(I) acetylide groups at the selective sites of the planar anthracene on the photophysical properties.

4. Experimental

4.1. General methods

All manipulations were carried out at room temperature under a nitrogen atmosphere. Solvents were predried, distilled and degassed prior to use, except those for spectroscopic measurements, which were of spectroscopic grade. The starting materials 9,10-dibromoanthracene, 1,8-diidoanthracene and AuPPh_3Cl were commercially available. The starting material 2,6-diidoanthracene was prepared by the procedures described in the literature [67] 9,10-Bis(trimethylsilyl)ethynyl anthracene [59,68–70], 2,6-Bis(trimethylsilyl)ethynyl anthracene [59,71], 1,8-Bis(trimethylsilyl)ethynyl anthracene [59,72,73], and their corresponding acetylenes were synthesized by earlier reported method [27].

4.2. Instruments

Elemental analyses were carried out with a Flash 2000 elemental analyzer. UV/Vis absorption and emission spectra were recorded on a Cary-100 Bio UV–Vis spectrophotometer and a Horiba Jobin-Yvon Fluoromax 4P spectrophotometer respectively. 9,10-bis(phenylethynyl) anthracene was used as a standard in measuring the quantum yields. ^1H NMR and ^{31}P NMR spectra were recorded on Bruker Avance(III) 400 MHz spectrometer. HRMS was recorded on a Brucker-Daltonics, micrOTOF-Q II mass spectrometer. Single-crystal X-ray structural studies were performed on an Agilent Technology Supernova CCD diffractometer equipped with a low-temperature attachment.

4.3. X-ray crystallography

Data were collected at 150 K for **2** and at 293 K for **1** and **3** using graphite-monochromated $\text{Mo K}\alpha$ ($\lambda\alpha = 0.71073 \text{ \AA}$) and $\text{Cu K}\alpha$ ($\lambda\alpha = 1.54814 \text{ \AA}$). The strategy for data collection was evaluated using the CrysAlisPro CCD software. The data were collected by the standard $\phi-\omega$ scan techniques and scaled and reduced using CrysAlisPro RED software. The structures were solved by direct methods using SHELXS-97 and refined by full-matrix least squares with SHELXL-97 on F^2 [74]. The positions of all of the atoms were obtained by direct methods. All non-H atoms were refined

Table 1
Absorption and emission spectroscopic details of **1**, **2** and **3**.

S. No	Absorption λ_{\max} nm $10^{-5}/\epsilon_{\max}$ ($\text{cm}^{-1}, \text{M}^{-1}$)	Emission λ_{\max} (nm)	Emission life time (τ)ns	Quantum yield Φ
1	462(1.01), 434(0.781), 410(0.387), 275(1.87), 230(2.07)	499	4.06	0.89
2	412(1.17), 389(1.36), 366(0.897), 310(8.77), 238(4.30)	445	4.02	0.02
3	422(0.976), 398(0.936), 376(0.583), 267(5.67), 228(4.69)	455	0.57	0.038

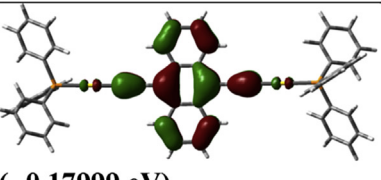
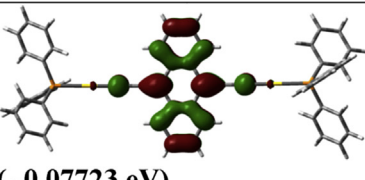
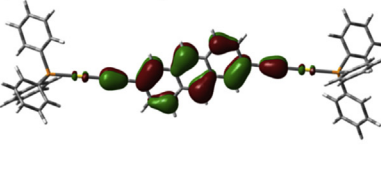
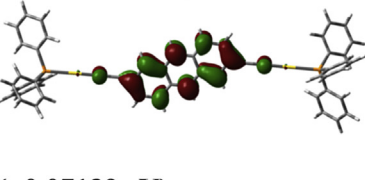
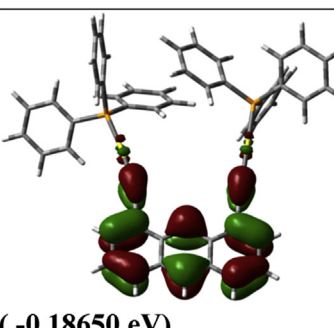
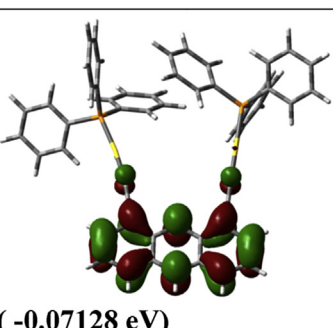
	HOMO	LUMO	Band Gap
1			0.10276(eV)
2			0.11725(eV)
3			0.11538(eV)

Fig. 10. HOMO and LUMO of complexes **1**, **2** and **3** and their band gap.

anisotropically. In **3** SQUEEZE was applied by using platon programme to remove disorder chloroform solvent molecules. All Hydrogen atoms were placed in geometrically constrained position and refined with isotropic temperature factors, generally $1.2 \times U_{eq}$ of their parent atoms. Moreover, despite several attempts we could not get better quality of crystals for **2** and **3**. All the short contacts and interactions, mean-plane analyses, and molecular drawings were obtained using the Diamond program (version 3.1d) and Mercury (v 3.5.1). The crystal and refinement data are summarized in Table S1, and selected bond distances and angles are shown in Table S2.

4.4. Synthesis of $(Ph_3PAu^I)_2\text{-}9,10\text{-anthracenyldiacetylide } \mathbf{1}$

To a suspension of Ph_3PAuCl (100 mg, 0.20 mmol) in ethanol (20 ml) $NaOEt$, freshly prepared from sodium (4.87 mg, 0.21 mmol) in ethanol (5 ml) and 9,10-bis(ethynylanthracene) (22.6 mg, 0.10 mmol) were added. The solution was refluxed for 1 h, cooled and concentrated after which a yellow precipitate formed. The yellow colored solid was isolated by simple filtration method. The precipitate was further washed with ethanol and dried at room temperature to afford **1**. X-ray quality crystals of **1** were obtained from $CHCl_3/\text{hexane}$ at room temperature. Yield: 60% Anal Calcd for **1** ($C_{54}H_{38}Au_2P_2$) C 56.76, H 3.35. Found: C 56.81, H 3.05 ^1H NMR (400 MHz, $CDCl_3$) δ = 8.86 (dd, J = 3.2, 4H ant), 7.49–7.65 (m, 34H anth and PPh_3), ^{13}C NMR (100 MHz, $CDCl_3$) δ = 96.51, 125.73, 128.17, 129.14, 129.26, 131.58, 132.79, 134.36, 134.49, ^{31}P NMR (165.561 MHz, $CDCl_3$) 42.38 ESI-MS: 1142[M].

4.5. Synthesis of $(Ph_3PAu^I)_2\text{-}2,6\text{-anthracenyldiacetylide } \mathbf{2}$

Complex **2** was synthesized by following the same method as **1**

using 2,6-bis(ethynylanthracene). Light yellow color crystals of **2** were grown in CH_2Cl_2/hexane at room temperature. Yield: 38% Anal Calcd for **2** ($C_{54}H_{38}Au_2P_2$) C 56.76, H 3.35. Found: C 57.12, H 2.89 ^1H NMR (400 MHz, $CDCl_3$) δ = 8.22 (s, 2H ant), 8.13 (s, 2H ant), 7.85 (d, J = 10.28, 2H ant), 7.45–7.60 (m, 32H ant and PPh_3), ^{13}C NMR (100 MHz, $CDCl_3$) δ = 91.92, 125.56, 127.71, 129.13, 129.24, 129.35, 130.72, 131.58, 131.93, 134.29, 134.43, ^{31}P NMR (165.561 MHz, $CDCl_3$) 42.31 ESI-MS: 1142[M].

4.6. Synthesis of $(Ph_3PAu^I)_2\text{-}1,8\text{-anthracenyldiacetylide } \mathbf{3}$

Complex **3** was synthesized by following the method described above for **1** using 1,8-bis(ethynyl anthracene). Golden yellow color crystals of **3** were grown in $CHCl_3/\text{hexane}$ at room temperature. Yield: 48% Anal Calcd for **3** ($C_{54}H_{38}Au_2P_2$) C 56.76, H 3.209. Found: C 57.01, H 3.508 ^1H NMR (400 MHz, $CDCl_3$) δ = 9.83 (s 1H anthracene), 8.35 (s 1H anthracene) 7.86 (d, J = 8.5, 2H ant), 7.80 (d, J = 6.7, 2H ant), 7.54–7.47 (m, 32H ant and PPh_3), ^{13}C NMR (100 MHz, $CDCl_3$) δ = 87.56, 124.96, 126.90, 127.22, 129.01, 129.12, 130.35, 131.34, 131.57, 132.07, 134.33, 134.46, ^{31}P NMR (165.561 MHz, $CDCl_3$) 42.19 ESI-MS: 1165[M + 23].

Acknowledgements

We are grateful for the use of the Single Crystal X-ray diffraction facility at the Sophisticated Instrumentation Centre (SIC), IIT Indore. SMM thanks CSIR, New Delhi, for a research grant.

Appendix A. Supplementary data

Supplementary data related to this article can be found at <http://dx.doi.org/10.1016/j.jorgchem.2016.04.013>.

References

- [1] J. Zaumseil, H. Sirringhaus, Chem. Rev. 107 (2007) 1296.
- [2] S.-C. Lo, P.L. Burn, Chem. Rev. 107 (2007) 1097.
- [3] J.E. Anthony, Angew. Chem. Int. Ed. 47 (2008) 452.
- [4] R. Ruiz, D. Choudhary, B. Nickel, T. Toccoli, K.-C. Chang, A.C. Mayer, P. Clancy, J.M. Blakely, R.L. Headrick, S. Iannotta, G.G. Malliaras, Chem. Mater. 16 (2004) 4497.
- [5] M. Bendikov, F. Wudl, D.F. Perepichka, Chem. Rev. 104 (2004) 4891.
- [6] D.W. Bruce, D.O. Hare, Inorganic Materials, John Wiley & Sons Ltd, Chichester, 1996.
- [7] N.J. Long, Angew. Chem. Int. Ed. 34 (1995) 21.
- [8] N.J. Long, C.K. Williams, Angew. Chem. Int. Ed. 42 (2003) 2586.
- [9] M.-H. Nguyen, J.H.K. Yip, Organometallics 29 (2010) 2422.
- [10] J. Hu, R. Lin, J.H.K. Yip, K.-Y. Wong, D.-L. Ma, J.J. Vittal, Organometallics 26 (2007) 6533.
- [11] J. Hu, J.H.K. Yip, D.-L. Ma, K.-Y. Wong, W.-H. Chung, Organometallics 28 (2009) 51.
- [12] J. Hu, H. Xu, M.-H. Nguyen, J.H.K. Yip, Inorg. Chem. 48 (2009) 9684.
- [13] W.Y. Heng, J. Hu, J.H.K. Yip, Organometallics 26 (2007) 6760.
- [14] B.-Y. Wang, A.R. Karikachery, Y. Li, A. Singh, H.B. Lee, W. Sun, P.R. Sharp, J. Am. Chem. Soc. 131 (2009) 3150.
- [15] L.-L. Hung, W.H. Lam, K.M.-C. Wong, E.C.-C. Cheng, N. Zhu, V.W.-W. Yam, Inorg. Chem. Front. 2 (2015) 453.
- [16] V.W.-W. Yam, E.C.-C. Cheng, Top. Curr. Chem. 281 (2007) 269.
- [17] V.W.-W. Yam, E.C.-C. Cheng, Chem. Soc. Rev. 37 (2008) 1806.
- [18] J. Hu, R. Lin, J.H.K. Yip, K.-Y. Wong, D.-L. Ma, J.J. Vittal, Organometallics 26 (2007) 6533.
- [19] J. Hu, J.H.K. Yip, D.-L. Ma, K.-Y. Wong, W.-H. Chung, Organometallics 28 (2009) 51.
- [20] J. Hu, H. Xu, M.-H. Nguyen, J.H.K. Yip, Inorg. Chem. 48 (2009) 9684.
- [21] J. Hu, J.H.K. Yip, Organometallics 28 (2009) 1093.
- [22] W.-Y. Wong, C.-L. Ho, Coord. Chem. Rev. 250 (2006) 2627.
- [23] M.-H. Nguyen, J.H.K. Yip, Organometallics 29 (2010) 2422.
- [24] T. Müller, S.W.K. Choi, D.M.P. Mingos, D. Murphy, D.J. Williams, V.W.-W. Yam, J. Organomet. Chem. 484 (1994) 209.
- [25] V.W.-W. Yam, S.W.K. Choi, J. Chem. Soc. Dalton Trans. (1996) 4227.
- [26] V.W.-W. Yam, S.W.K. Choi, K.K. Cheung, Organometallics 15 (1996) 1734.
- [27] H. Xiao, K.K. Cheung, C.M. Che, J. Chem. Soc. Dalton Trans. (1996) 3699.
- [28] M.J. Irwin, J.J. Vittal, R.J. Puddephatt, Organometallics 16 (1997) 3541.
- [29] V.W.-W. Yam, K.L. Cheung, L.H. Yuan, K.M.C. Wong, K.K. Cheung, Chem. Commun. 16 (2000) 1513.
- [30] V.W.-W. Yam, S.K. Yip, L.H. Yuan, K.L. Cheung, N. Zhu, K.K. Cheung, Organometallics 22 (2003) 2630.
- [31] V.W.-W. Yam, K.L. Cheung, S.K. Yip, K.K. Cheung, J. Organomet. Chem. 681 (2003) 196.
- [32] V.W.-W. Yam, K.L. Cheung, E.C.C. Cheng, N. Zhu, K.K. Cheung, J. Chem. Soc. Dalton Trans. (2003) 1830.
- [33] W. Lu, N. Zhu, C.M. Che, J. Am. Chem. Soc. 125 (2003) 16081.
- [34] J.S. Ovens, K.N. Truong, D.B. Leznoff, Dalton Trans. 41 (2012) 1345.
- [35] E.S. Kryachko, J. Mol. Struct. 880 (2008) 114.
- [36] A. Martínez, J. Phys. Chem. A 113 (2009) 1134.
- [37] T.V. Baukova, L.G. Kuz'mina, N.A. Oleinikova, D.A. Lemenovskii, A.L. Blumenfeld, J. Organomet. Chem. 530 (1997) 27.
- [38] A. Castineiras, N. Fernandez-Hermida, R. Fernandez-Rodríguez, I. García-Santos, Cryst. Growth. Des. 12 (2012) 1432.
- [39] L.-I. Rodríguez, T. Roth, J.L. Fillol, H. Wadeppohl, L.H. Gade, Chem. Eur. J. 18 (2012) 3721.
- [40] M. Friki, J. Jimenez, I. Gracia, L.R. Falvello, S. Abi-Habib, K. Suriel, T.R. Muth, M. Contel, Chem. Eur. J. 18 (2012) 3659.
- [41] M. Hejda, L. Dostál, R. Jambor, A. Ruzicka, R. Jirasko, J. Holecek, Eur. J. Inorg. Chem. (2012) 2578.
- [42] Y.-P. Zhou, M. Zhang, Y.-H. Li, Q.-R. Guan, F. Wang, Z.-J. Lin, C.-K. Lam, X.-L. Feng, H.-Y. Chao, Inorg. Chem. 51 (2012) 5099.
- [43] H. Nuss, M.Z. Jansen, Naturforsch 61b (2006) 1205.
- [44] H. Nuss, M. Jansen, Angew. Chem. Int. Ed. 45 (2006) 4369.
- [45] P.D.C. Dietzel, M. Jansen, Chem. Commun. (2001) 2208.
- [46] H. Schmidbaur, H.G. Raubenheimer, L. Dobrzenska, Chem. Soc. Rev. 43 (2014) 345.
- [47] K.J. Kilpin, R. Horvath, G.B. Jameson, S.G. Telfer, K.C. Gordon, J.D. Crowley, Organometallics 29 (2010) 6186.
- [48] G. Hogarth, M.M. Alvarez-Falcon, Inorg. Chim. Acta 358 (2005) 1386.
- [49] C. Croix, A. Balland-Longeau, H. Allouchi, M. Giorgi, A. Duchene, J. Thibonnet, J. Organomet. Chem. 690 (2005) 4835.
- [50] V.W.-W. Yam, K.-L. Cheung, S.-K. Yip, N. Zhu, Photochem. Photobiol. Sci. 4 (2005) 149.
- [51] L. Koskinen, S. Jääskeläinen, E. Kalenius, P. Hirva, M. Haukka, Cryst. Growth. Des. 14 (2014) 1989.
- [52] A.K. Bar, S. Shamugaraju, K.-W. Chi, P.S. Mukherjee, Dalton Trans. 40 (2011) 2257.
- [53] S. Ghosh, R. Chakrabarty, P.S. Mukherjee, Inorg. Chem. 48 (2009) 549.
- [54] A.K. Bar, B. Gole, S. Ghosh, P.S. Mukherjee, Dalton. Trans. (2009) 6701.
- [55] C.-H. Tao, N. Zhu, V.W.-W. Yam, Chem. Eur. J. 11 (2005) 1647.
- [56] M. Kessinger, J. Michl, Excited States and Photochemistry of Organic Molecules, VCH, New York, 1995.
- [57] M.-H. Nguyen, C.-Y. Wong, J.H.K. Yip, Organometallics 32 (2013) 1620.
- [58] N. Agarwal, M. Patil, M. Patil, RSC Adv. 5 (2015) 98447.
- [59] Y.-P. Ou, C. Jiang, D. Wu, J.Y. Xia, S. Jin, G.-A. Yu, S.H. Liu, Organometallics 30 (2011) 5763.
- [60] M.J. Frisch, G.W. Trucks, H.B. Schlegel, G.E. Scuseria, M.A. Robb, J.R. Cheeseman, G. Scalmani, V. Barone, B. Mennucci, G.A. Petersson, H. Nakatsuji, M. Caricato, X. Li, H.P. Hratchian, A.F. Izmaylov, J. Bloino, G. Zheng, J.L. Sonnenberg, M. Hada, M. Ehara, K. Toyota, R. Fukuda, J. Hasegawa, M. Ishida, T. Nakajima, Y. Honda, O. Kitao, H. Nakai, T. Vreven, J.A. Montgomery Jr., J.E. Peralta, F. Ogliaro, M. Bearpark, J.J. Heyd, E. Brothers, K.N. Kudin, V.N. Staroverov, R. Kobayashi, J. Normand, K. Raghavachari, A. Rendell, J.C. Burant, S.S. Iyengar, J. Tomasi, M. Cossi, N. Rega, N.J. Millam, M. Klene, J.E. Knox, J.B. Cross, V. Bakken, C. Adamo, J. Jaramillo, R. Gomperts, R.E. Stratmann, O. Yazyev, A.J. Austin, R. Cammi, C. Pomelli, J.W. Ochterski, R.L. Martin, K. Morokuma, V.G. Zakrzewski, G.A. Voth, P. Salvador, J.J. Dannenberg, S. Dapprich, A.D. Daniels, Ö. Farkas, J.B. Foresman, J.V. Ortiz, J. Cioslowski, D.J. Fox, Gaussian 09, Revision D.01, Gaussian, Inc., Wallingford, CT, 2009.
- [61] A.D. Becke, J. Chem. Phys. 98 (1993) 5648.
- [62] C. Lee, W. Yang, R.G. Parr, Phys. Rev. B Condens. Matter 37 (1988) 785.
- [63] T.H. Dunning Jr., P.J. Hay, Modern Theoretical Chemistry 3, Plenum, New York, 1976.
- [64] R. Ditchfield, W.J. Hehre, A. Pople, J. Chem. Phys. 54 (1971) 724.
- [65] V. Barone, M. Cossi, J. Phys. Chem. A 102 (1998) 1995.
- [66] M. Cossi, N. Rega, G. Scalmani, V. Barone, J. Comput. Chem. 24 (2003) 669.
- [67] M.T. Stone, H.L. Anderson, Chem. Commun. (2007) 2387.
- [68] W. Fudickar, T. Linker, J. Am. Chem. Soc. 134 (2012) 15071.
- [69] J. Kaleta, E. Kaletová, I. Číšarová, S.J. Teat, J. Michl, J. Org. Chem. 80 (2015) 10134.
- [70] Y. Li, M.E. Köse, K.S. Schanze, J. Phys. Chem. B 117 (2013) 9025.
- [71] Y. Sagara, S. Yamane, T. Mutai, K. Araki, T. Kato, Adv. Funct. Mater. 19 (2009) 1869.
- [72] M. Pauvert, P. Laine, M. Jonas, O. Wiest, J. Org. Chem. 69 (2004) 543.
- [73] J.-H. Lamm, J. Glatthor, J.-H. Weddeling, A. Mix, J. Chmiel, B. Neumann, H.-G. Stamm, N.W. Mitzel, Org. Biomol. Chem. 12 (2014) 7355.
- [74] G.M. Sheldrick, Acta Crystallogr. Sect. A A64 (2008) 112. Program for Crystal Structure Solution and Refinement; University of Göettingen: Göettingen, Germany, 1997.